Search for Baryon and Lepton Number Violating Z^0 Decays

The OPAL Collaboration

Abstract

Using data collected with the OPAL detector at LEP, we have searched for the processes $e^+e^- \rightarrow Z^0 \rightarrow pe^-, p\mu^-$ and the charge conjugate final-states. These would violate the conservation of the baryon-number B, lepton-number L and the fermion-number n = (B+L). No evidence for such decays has been found, and the 95 % confidence level upper limits on the partial widths $\Gamma(Z^0 \rightarrow pe)$ and $\Gamma(Z^0 \rightarrow p\mu)$ are found to be 4.6 and 4.4 keV respectively.

(Submitted to Physics Letters B)

The OPAL Collaboration

G. Abbiendi[2], K. Ackerstaff[8], G. Alexander[23], J. Allison[16], N. Altekamp[5], K.J. Anderson[9], S. Anderson[12], S. Arcelli[17], S. Asai[24], S.F. Ashby[1], D. Axen[29], G. Azuelos[18,a], A.H. Ball[17], E. Barberio[8], R.J. Barlow[16], R. Bartoldus[3], J.R. Batley[5], S. Baumann[3], J. Bechtluft[14], T. Behnke[27], K.W. Bell[20], G. Bella[23], A. Bellerive[9], S. Bentvelsen[8], S. Bethke[14], S. Betts[15], O. Biebel[14], A. Biguzzi[5], S.D. Bird[16], V. Blobel[27], I.J. Bloodworth[1], P. Bock[11], J. Böhme[14], D. Bonacorsi[2], M. Boutemeur[34], S. Braibant[8], P. Bright-Thomas[1], L. Brigliadori[2], R.M. Brown[20], H.J. Burckhart[8], P. Capiluppi[2], R.K. Carnegie[6], A.A. Carter[13], J.R. Carter[5], C.Y. Chang[17], D.G. Charlton[1,b], D. Chrisman[4], C. Ciocca[2], P.E.L. Clarke[15], E. Clay[15], I. Cohen[23], J.E. Conboy[15], O.C. Cooke[8], C. Couyoumtzelis[13], R.L. Coxe[9], M. Cuffiani[2], S. Dado[22], G.M. Dallavalle[2], R. Davis[30], S. De Jong[12], A. de Roeck[8], P. Dervan[15], K. Desch[8], B. Dienes[33,d], M.S. Dixit[7], J. Dubbert[34], E. Duchovni[26], G. Duckeck[34], I.P. Duerdoth[16], D. Eatough[16], P.G. Estabrooks[6], E. Etzion[23], F. Fabbri[2], M. Fanti[2], A.A. Faust[30], F. Fiedler[27], M. Fierro[2], I. Fleck[8], R. Folman[26], A. Fürtjes[8], D.I. Futyan[16], P. Gagnon[7], J.W. Gary[4], J. Gascon[18], S.M. Gascon-Shotkin[17], G. Gaycken[27], C. Geich-Gimbel[3], G. Giacomelli[2], P. Giacomelli[2], V. Gibson[5], W.R. Gibson[13], D.M. Gingrich[30,a], D. Glenzinski[9], J. Goldberg[22], W. Gorn[4], C. Grandi[2], K. Graham[28], E. Gross[26], J. Grunhaus[23], M. Gruwé[27], G.G. Hanson[12], M. Hansroul[8], M. Hapke[13], K. Harder[27], A. Harel[22], C.K. Hargrove[7], C. Hartmann[3], M. Hauschild[8], C.M. Hawkes[1], R. Hawkings[27], R.J. Hemingway[6], M. Herndon[17], G. Herten[10], R.D. Heuer[27], M.D. Hildreth[8], J.C. Hill[5], P.R. Hobson[25], M. Hoch[18], A. Hocker[9], K. Hoffman[8], R.J. Homer[1], A.K. Honma[28,a], D. Horváth[32,c], K.R. Hossain[30], R. Howard[29], P. Hüntemeyer[27], P. Igo-Kemenes[11], D.C. Imrie[25], K. Ishii[24], F.R. Jacob[20], A. Jawahery[17], H. Jeremie[18], M. Jimack[1], C.R. Jones[5], P. Jovanovic[1], T.R. Junk[6], D. Karlen[6], V. Kartvelishvili[16], K. Kawagoe[24], T. Kawamoto[24], P.I. Kayal[30], R.K. Keeler[28], R.G. Kellogg[17], B.W. Kennedy[20], D.H. Kim[19], A. Klier[26], S. Kluth[8], T. Kobayashi[24], M. Kobel[3,e], D.S. Koetke[6], T.P. Kokott[3], M. Kolrep[10], S. Komamiya[24], R.V. Kowalewski[28], T. Kress[4], P. Krieger[6], J. von Krogh[11], T. Kuhl[3], P. Kyberd[13], G.D. Lafferty[16], H. Landsman[22], D. Lanske[14], J. Lauber[15], S.R. Lautenschlager[31], I. Lawson[28], J.G. Layter[4], D. Lazic[22], A.M. Lee[31], D. Lellouch[26], J. Letts[12], L. Levinson[26], R. Liebisch[11], B. List[8], C. Littlewood[5], A.W. Lloyd[1], S.L. Lloyd[13], F.K. Loebinger[16], G.D. Long[28], M.J. Losty[7], J. Ludwig[10], D. Liu[12], A. Macchiolo[2], A. Macpherson[30], W. Mader[3], M. Mannelli[8], S. Marcellini[2], C. Markopoulos[13], A.J. Martin[13], J.P. Martin[18], G. Martinez[17], T. Mashimo[24], P. Mättig[26], W.J. McDonald[30], J. McKenna[29], E.A. Mckigney[15], T.J. McMahon[1], R.A. McPherson[28], F. Meijers[8], S. Menke[3], F.S. Merritt[9], H. Mes[7], J. Meyer[27], A. Michelini[2], S. Mihara[24], G. Mikenberg[26], D.J. Miller[15], R. Mir[26], W. Mohr[10], A. Montanari[2], T. Mori[24], K. Nagai[8], I. Nakamura[24], H.A. Neal[12], B. Nellen[3], R. Nisius[8], S.W. O'Neale[1], F.G. Oakham[7], F. Odorici[2], H.O. Ogren[12], M.J. Oreglia[9], S. Orito[24], J. Pálinkás[33,d], G. Pásztor[32], J.R. Pater[16], G.N. Patrick[20], J. Patt[10], R. Perez-Ochoa[8], S. Petzold[27], P. Pfeifenschneider[14], J.E. Pilcher[9], J. Pinfold[30], D.E. Plane[8], P. Poffenberger[28], J. Polok[8], M. Przybycień[8], C. Rembser[8], H. Rick[8], S. Robertson[28], S.A. Robins[22], N. Rodning[30], J.M. Roney[28], K. Roscoe[16], A.M. Rossi[2], Y. Rozen[22], K. Runge[10], O. Runolfsson[8], D.R. Rust[12], K. Sachs[10], T. Saeki[24], O. Sahr[34], W.M. Sang[25], E.K.G. Sarkisyan[23], C. Sbarra[29], A.D. Schaile[34], O. Schaile[34], F. Scharf[3], P. Scharff-Hansen[8], J. Schieck[11], B. Schmitt[8], S. Schmitt[11], A. Schöning[8], M. Schröder[8], M. Schumacher[3], C. Schwick[8], W.G. Scott[20], R. Seuster[14], T.G. Shears[8], B.C. Shen[4], C.H. Shepherd-Themistocleous[8], P. Sherwood[15], G.P. Siroli[2], A. Sittler[27], A. Skuja[17], A.M. Smith[8], G.A. Snow[17], R. Sobie[28], S. Söldner-Rembold[10],

S. Spagnolo[20], M. Sproston[20], A. Stahl[3], K. Stephens[16], J. Steuerer[27], K. Stoll[10], D. Strom[19], R. Ströhmer[34], B. Surrow[8], S.D. Talbot[1], S. Tanaka[24], P. Taras[18], S. Tarem[22], R. Teuscher[8], M. Thiergen[10], J. Thomas[15], M.A. Thomson[8], E. von Törne[3], E. Torrence[8], S. Towers[6], I. Trigger[18], Z. Trócsányi[33], E. Tsur[23], A.S. Turcot[9], M.F. Turner-Watson[1], I. Ueda[24], R. Van Kooten[12], P. Vannerem[10], M. Verzocchi[10], H. Voss[3], F. Wäckerle[10], A. Wagner[27], C.P. Ward[5], D.R. Ward[5], P.M. Watkins[1], A.T. Watson[1], N.K. Watson[1], P.S. Wells[8], N. Wermes[3], J.S. White[6], G.W. Wilson[16], J.A. Wilson[1], T.R. Wyatt[16], S. Yamashita[24], G. Yekutieli[26], V. Zacek[18], D. Zer-Zion[8]

[1]School of Physics and Astronomy, University of Birmingham, Birmingham B15 2TT, UK

[2]Dipartimento di Fisica dell' Università di Bologna and INFN, I-40126 Bologna, Italy

[3]Physikalisches Institut, Universität Bonn, D-53115 Bonn, Germany

[4]Department of Physics, University of California, Riverside CA 92521, USA

[5]Cavendish Laboratory, Cambridge CB3 0HE, UK

[6]Ottawa-Carleton Institute for Physics, Department of Physics, Carleton University, Ottawa, Ontario K1S 5B6, Canada

[7]Centre for Research in Particle Physics, Carleton University, Ottawa, Ontario K1S 5B6, Canada

[8]CERN, European Organisation for Particle Physics, CH-1211 Geneva 23, Switzerland

[9]Enrico Fermi Institute and Department of Physics, University of Chicago, Chicago IL 60637, USA

[10]Fakultät für Physik, Albert Ludwigs Universität, D-79104 Freiburg, Germany

[11]Physikalisches Institut, Universität Heidelberg, D-69120 Heidelberg, Germany

[12]Indiana University, Department of Physics, Swain Hall West 117, Bloomington IN 47405, USA

[13]Queen Mary and Westfield College, University of London, London E1 4NS, UK

[14]Technische Hochschule Aachen, III Physikalisches Institut, Sommerfeldstrasse 26-28, D-52056 Aachen, Germany

[15]University College London, London WC1E 6BT, UK

[16]Department of Physics, Schuster Laboratory, The University, Manchester M13 9PL, UK

[17]Department of Physics, University of Maryland, College Park, MD 20742, USA

[18]Laboratoire de Physique Nucléaire, Université de Montréal, Montréal, Quebec H3C 3J7, Canada

[19]University of Oregon, Department of Physics, Eugene OR 97403, USA

[20]CLRC Rutherford Appleton Laboratory, Chilton, Didcot, Oxfordshire OX11 0QX, UK

[22]Department of Physics, Technion-Israel Institute of Technology, Haifa 32000, Israel

[23]Department of Physics and Astronomy, Tel Aviv University, Tel Aviv 69978, Israel

[24]International Centre for Elementary Particle Physics and Department of Physics, University of Tokyo, Tokyo 113-0033, and Kobe University, Kobe 657-8501, Japan

[25]Institute of Physical and Environmental Sciences, Brunel University, Uxbridge, Middlesex UB8 3PH, UK

[26]Particle Physics Department, Weizmann Institute of Science, Rehovot 76100, Israel

[27]Universität Hamburg/DESY, II Institut für Experimental Physik, Notkestrasse 85, D-22607 Hamburg, Germany

[28]University of Victoria, Department of Physics, P O Box 3055, Victoria BC V8W 3P6, Canada

[29]University of British Columbia, Department of Physics, Vancouver BC V6T 1Z1, Canada

[30]University of Alberta, Department of Physics, Edmonton AB T6G 2J1, Canada
[31]Duke University, Dept of Physics, Durham, NC 27708-0305, USA
[32]Research Institute for Particle and Nuclear Physics, H-1525 Budapest, P O Box 49, Hungary
[33]Institute of Nuclear Research, H-4001 Debrecen, P O Box 51, Hungary
[34]Ludwigs-Maximilians-Universität München, Sektion Physik, Am Coulombwall 1, D-85748 Garching, Germany

[a] and at TRIUMF, Vancouver, Canada V6T 2A3
[b] and Royal Society University Research Fellow
[c] and Institute of Nuclear Research, Debrecen, Hungary
[d] and Department of Experimental Physics, Lajos Kossuth University, Debrecen, Hungary
[e] on leave of absence from the University of Freiburg

1 Introduction

No symmetry principle is known in physics which may guarantee the conservation of baryon (B)- or lepton (L)-number. Nevertheless, there are two important observations which are relevant to B and L non-conservation in a very profound way: namely baryogenesis [1], and the realization that B and L are not strictly conserved in the Standard Model of electroweak interactions [2].

In the standard hot big bang model [3], one of the most obvious relics from the early universe is the baryon. But the universe, at some distance scale around us, ℓ_B, is practically 100 % charge asymmetric, with baryon number density very much exceeding that of antibaryons, $n_B \gg n_{\bar{B}}$ (and $n_{e^-} \gg n_{e^+}$). The distance ℓ_B is at least of the size of our visible universe. The standard electroweak theory contains in principle all the elements necessary for the generation of the baryonic asymmetry of the universe [4, 5]. These theoretical elements are

(i) anomalous electroweak baryon-number non-conservation [2],

(ii) C- and CP-violation in the fundamental gauge and Higgs interactions of the quarks,

(iii) deviation from thermal equilibrium, assuming the cosmological electroweak phase transition is first order [5], which occurs at temperatures of about $\sim 100\,\mathrm{GeV}$.[1]

At low temperatures, this anomalous electroweak B violation is negligible [1, 6]. For instance, the proton lifetime, determined from the absence of the decay $\mathrm{p} \to \mathrm{e}^+ \mathrm{Z}^{0\star} \to \mathrm{e}^+ \mathrm{e}^+ \mathrm{e}^-$ was found to be larger than 5×10^{32} years at 90 % confidence level [7]. On the other hand, at the Z^0 resonance with an equivalent temperature of 90 GeV, the decays $\mathrm{Z}^0 \to \mathrm{pe}/\mathrm{p}\mu$ may conceivably occur at an observable level due to the anomalous interactions mentioned above.

In this paper, we present the results of a search for the decays $\mathrm{Z}^0 \to \mathrm{pe}^-, \mathrm{p}\mu^-$ and their charge conjugate final-states, $\bar{\mathrm{p}}\mathrm{e}^+$ and $\bar{\mathrm{p}}\mu^+$, with the OPAL detector at LEP. These decays would violate B, L and the fermion number, n = (B+L) while conserving (B–L). We have searched for events characterized by a pair of back-to-back charged particles, where one is identified as a lepton and the other as a proton. Although other rare decay modes of the Z^0 can also be handled in the same analysis, they are not discussed here since they either violate conservation laws attributable to some fundamental symmetries, or since stringent constraints on their rates have already been set by OPAL and other LEP experiments [8].

2 The OPAL detector and data sample

A complete description of the OPAL detector can be found in Ref. [9], and only those components most relevant to the identification of high energy electrons, muons and protons are described briefly here.

---

[1]Sakharov suggested [4] that baryogenesis took place immediately after the big bang, at a temperature not far below the Planck scale of 10^{19} GeV. This scenario was explicitly realized with the advent of the Grand Unified Theory (GUT), which predicts B and possibly CP violations, mediated by very heavy gauge bosons, X and Y. The GUT baryogenesis is appealingly simple but does not easily fit into an acceptable cosmology.

The central detector provides charged particle tracking over 96% of the full solid angle in a 0.435 T uniform magnetic field parallel to the beam axis [2]. It consists of a two-layer silicon microstrip vertex detector, a high precision drift chamber, a large volume jet chamber, and a set of z chambers measuring the track coordinates along the beam direction. The sensitive volume of the jet chamber is a cylinder of about 2 m in radius and 4 m in length. It is divided into 24 sectors, each equipped with 159 sense wires and two cathode wire planes. Up to 159 measurements of position and charge deposition per track are possible. The momentum resolution of the whole tracking system is $\sigma_{p_t}/p_t \approx \sqrt{0.02^2 + (0.0015 \cdot p_t)^2}$ where p_t is the momentum component transverse to the beam direction. The charge measurements were used for the calculation of the specific energy loss $d\mathrm{E}/dx$ of a track. The $d\mathrm{E}/dx$ resolutions obtained with a number of samplings $N > 130$ are = 3.1 % and 3.8 % for muons in $\mathrm{Z}^0 \to \mu^+\mu^-$ and for minimum ionising pions within jets, respectively [10]. A detailed description of the main features of the jet chamber can be found in [11].

The magnetic coil is surrounded by a time-of-flight counter array (TOF) which measures the time-of-flight for a charged particle from the interaction region with a time resolution of about 300 ps and can be used for the rejection of cosmic ray muons. A lead-glass electromagnetic calorimeter (ECAL), located outside the magnet coil, covers the full azimuthal range with excellent hermeticity in the polar angle range of $|\cos\theta| < 0.984$. In the barrel region ($|\cos\theta| < 0.82$), the ECAL is composed of 9440 lead-glass blocks, each 37 cm in depth. The blocks are approximately $10 \times 10\,cm^2$ in cross section, and the calorimeter is typically 24.6 radiation lengths deep. The energy resolution of the barrel ECAL is approximately $\sigma_E/E \simeq 2.3\%$ for 45 GeV electrons. The magnet return yoke is segmented and instrumented for hadron calorimetry (HCAL) and consists of barrel and endcap sections along with pole tip detectors that together cover the region $|\cos\theta| < 0.99$. The HCAL provides tracking for muons above $3\,\mathrm{GeV}$ and sampling for the showers produced by hadrons interacting with material (a total of ~ 8 absorption lengths to the back of HCAL in the barrel region) inside the lead glass of ECAL and the return yoke of HCAL. Four layers of muon chambers cover the outside of the hadron calorimeter.

The electromagnetic calorimeters close to the beam axis complete the geometrical acceptance down to 24 mrad in θ, except for the regions where a tungsten shield is present to protect the detectors from synchrotron radiation. These are lead-scintillator sandwich calorimeters and, at smaller angles, silicon tungsten calorimeters [12] located on both sides of the interaction point and used for luminosity measurement.

The data used for this analysis were recorded at LEP during 1990 – 1994. The integrated luminosity of the data sample is 119 pb^{-1} [13] corresponding to 5.2 million Z^0 decays.

3   Monte Carlo simulations

The simulation of $\mathrm{Z}^0 \to \mathrm{pe}^-, \mathrm{p}\mu^-$ decays and their charge conjugate final-states begins with 20,000 $\mathrm{Z}^0 \to \mu^+\mu^-$ events that were generated at the Z^0 resonance peak with $\sqrt{s} = 91.2$ GeV using the KORALZ [14] Monte Carlo. The masses, particle types and the four momenta vectors of the muon pairs were then changed into those of $\mathrm{pe}^-, \bar{\mathrm{p}}\mathrm{e}^+, \mathrm{p}\mu^-$ or $\bar{\mathrm{p}}\mu^+$ pairs with equal

---

[2]The OPAL coordinate system is defined so that the z axis is in the direction of the electron beam, the x axis is horizontal and points towards the centre of the LEP ring, and θ and ϕ are the polar and azimuthal angles, defined relative to the $+z$- and $+x$-axes, respectively. The radial coordinate is denoted as r.

probability and the necessary corrections were made to preserve momentum and energy conservation. Responses of the OPAL detector to these particles were then obtained by processing the four vectors through the OPAL Monte Carlo simulation chain [15].

The analysis procedure consists of the selection of a pair of collinear charged particles in the barrel region of the jet chamber, each with approximately the beam energy, followed by particle identification. Major backgrounds were anticipated from mis-identification of the high energy charged leptons in $Z^0 \rightarrow \mu^+\mu^-$, e^+e^-, and $\tau^+\tau^-$ decays. Large samples of Standard Model lepton pairs ($600\,000$ $\mu^+\mu^-$, $942\,000$ e^+e^- and $447\,500$ $\tau^+\tau^-$) were generated with the KORALZ and BABAMC [16] Monte Carlo programs. In addition, 1.3 million Standard Model Z^0 decays into q$\bar{q}$'s, where $q = u, d, c, s$ and b quarks, were also generated with the JETSET [17] Monte Carlo program. All events are then processed through the OPAL analysis chain [15].

4 Preselection

In this analysis, candidate events were chosen from a sample of low (charge) multiplicity events. We demanded that the events contained two, and only two, well–measured high energy tracks, satisfying the following preselection criteria to guarantee a high degree of redundancy in triggering and to give almost an 100 % trigger efficiency for the detection of the signal [18, 19]:

- Well–measured tracks were defined by:

    The distance of closest approach to the beam axis in the plane perpendicular to the beam axis must be less than 2 cm.

    The distance to the interaction point along the beam axis, at the point of closest approach in the plane transverse to the beam axis, must be less than 40 cm.

    The $\chi^2/n.d.f.$ of the track fit in the $r - \phi$ plane must be less than 2.

    The first sense wire in the jet chamber used for track fitting must lie within a radius of 75 cm from the colliding beam axis.

    There must be at least 100 hits used for the ionization energy loss, $d\mathrm{E}/dx$, measurement and 4 hits in the z chambers.

    The track polar angle must satisfy $|\cos\theta| < 0.7$.

    The track must have either its measured $p_t \geq 15\,\mathrm{GeV}/c$, or its associated $E_{ECAL} > 35\,\mathrm{GeV}$.

- To select the required event topology, the two tracks were required to be:

    oppositely charged and collinear within $\delta\theta_{acol} < 10°$,

    in coincidence at the TOF counters, where we demanded that:

    $$|t_1 sin\theta_1 - t_2 sin\theta_2| < 10 \text{ nsec}$$

    where $t_{1,2}$ and $\theta_{1,2}$ are the measured time-of-flights and polar angles of the two preselected particles respectively.

At this stage 139 328 events passed the event preselection criteria. Possible contamination from two photon interactions were efficiently removed by the high p_t and E_{ECAL} cuts. Cosmic muons passing through the interaction region were rejected by the coincidence requirement on their TOF measurements. The surviving events, consistent with the number expected from standard model Z^0 decays to e^+e^-, $\mu^+\mu^-$ and $\tau^+\tau^-$, constituted the major background to the signal. Comparisons of the data with these Standard Model Monte Carlo simulated Z^0 decay backgrounds are shown in row 3 of Table 1 for the numbers of events that survived preselection, and in Figures 1 and 2 for the $E_{tot} = E_{ECAL} + E_{HCAL}$ and $d\mathrm{E}/dx$ distributions of the charged tracks, respectively. The Monte Carlo simulated background reproduced the data very well.

5 Particle identification

We demanded, among the two pre-selected high energy particles in each event, that there be one identified charged lepton and one charged track identified as a proton and not as a lepton. Particle identification was achieved using five independent quantities, namely momentum (p), ionization energy loss ($d\mathrm{E}/dx$), energy deposits in the calorimeters, E_{ECAL} and E_{HCAL}, and the information on matching of muon chamber hits to the charged track. We defined a 'tracking road' along the direction of each charged track in the OPAL calorimeters with a width:

$$20\,\mathrm{mrad} + 100\,\mathrm{mrad}/p\,(\,\mathrm{GeV}/c), \text{ in HCAL}$$

$$100\,\mathrm{mrad} + 100\,\mathrm{mrad}/p\,(\,\mathrm{GeV}/c), \text{ in the muon chambers.}$$

- Electron identification:

    Electron candidates were defined as those tracks having $E_{ECAL} > 35\,\mathrm{GeV}$ with $E_{ECAL}/p > 0.8$, and no hits found in the 'tracking road', except for the first layer of the HCAL.

- Muon identification:

    As muon candidates we considered those tracks which failed the electron identification. Those tracks must have its measured momentum, p, satisfying $40\,\mathrm{GeV}/c < p < 60\,\mathrm{GeV}/c$, and have more than 4 hits along the 'tracking road'. To distinguish muons from protons, we further demanded that either at least two of the hits on the 'tracking road' be in the muon chamber, or there be at least 4 of the hits in the HCAL with no more than one hit per layer, or that there be at least 2 of the hits in the 3 outermost layers of the HCAL.

- Proton identification:

    We considered those tracks as proton candidates which failed the electron identification. The proton track must have $40\,\mathrm{GeV}/c < p < 60\,\mathrm{GeV}/c$ and have at least one hit found in HCAL with the expected total calorimeter energy associated with the measured track $E_{tot} > 10\,\mathrm{GeV}$, but requiring that $E_{ECAL} \leq 35\,\mathrm{GeV}$.

- Event identification:

    Finally, events identified as e^+e^- or $\mu^+\mu^-$ pairs were removed, while event to be identified as a signal must satisfy the $d\mathrm{E}/dx$ requirement defined below:

- $d\mathrm{E}/dx$ requirement:

  The proton must have a measured $d\mathrm{E}/dx < 9$ keV/cm (see Figure 2). For the accompanied e or μ, the measured $d\mathrm{E}/dx$ must agree with its expected value for the particle assignment and the measured momentum.

No events in the data sample survived the selection criteria, while 1.2 background events were expected from the Standard Model background processes.

6   Efficiency and systematic errors

To estimate the detection efficiency of the signal and to investigate possible bias in the selection of events, preselection and particle identification criteria were applied to reconstructed Monte Carlo signal events. The shaded histogram in Figure 1, with arbitrary normalization, shows the distribution of the expected total calorimeter energy, E_{tot}, associated with each of the measured tracks of pre-selected Monte Carlo simulated signal events. The low energy peak centered at 3 GeV comes from the muons, while the peak centered at the beam energy (45 GeV) comes from the electrons. The broad peak in the middle of the spectrum comes from the protons [15, 20]. No such central region broad peak is seen either in the data (points) or in the Monte Carlo simulated background (open histogram) events as shown in Figure 1.

The preselection criteria limited the acceptance of the signal to the barrel region of the OPAL detector where the jet chamber provided a large number of hits for each of the pre-selected charged tracks for the $d\mathrm{E}/dx$ and momentum measurements. These criteria ensured a better than 5.3 % resolution in momentum and a 3.5 % resolution on $d\mathrm{E}/dx$ for a 45 GeV charged particle. As a result, 3σ separation between protons and muons, and 4σ separation between protons and electrons at 45 GeV were achieved [10]. The $d\mathrm{E}/dx$ distribution of the pre-selected data is compared to that of the Monte Carlo simulated background in Figure 2. The shaded histogram shows the $d\mathrm{E}/dx$ distribution expected for 45 GeV protons. A $d\mathrm{E}/dx < 9$ keV/cm cut was used for the identification of protons.

Table 1 summarizes the event flow history. The equivalent integrated luminosities of the Monte Carlo generated background sample sizes are shown in row 1. Row 2 shows the numbers of these events, normalized to the recorded luminosity (119pb^{-1}), surviving the requirements of low (charge) multiplicity. In row 3, the numbers of Monte Carlo simulated events and data events surviving the preselection are compared. The agreement here is excellent. Not shown in the Table are the corresponding numbers for the standard model Monte Carlo simulated multi-hadronic decays of the Z^0, because we found that none of the 1.3 million Monte Carlo simulated $Z^0 \rightarrow q\bar{q}$ events survived the preselection criteria. In addition, six million Standard Model Z^0 decays were generated with JETSET [17] and subjected to a preselection at the four-vector level. We found no event other than the Standard Model $e^+e^-, \mu^+\mu^-$ or $\tau^+\tau^-$ pairs that survived the preselection criteria. In Table 1, row 4 shows that:

the pre-selected data were dominated by (97.4 %) $e^+e^-, \mu^+\mu^-$ pairs.

after preselection, the efficiency for the identification of e^+e^- was found to be 99.9 %, and 94.5 % for $\mu^+\mu^-$.

after the identified e^+e^- and $\mu^+\mu^-$ pairs were removed, none of the events in the data sample survived the $d\mathrm{E}/d\mathrm{x}$ requirement selection, while 1.2 events were expected from the simulated background.

the detection efficiencies of the signal events for $Z^0 \to \mathrm{p}\mu$ and pe, were found to be:
$\epsilon_{\mathrm{p}\mu} = 0.353 \pm 0.006(stat)$ and $\epsilon_{\mathrm{pe}} = 0.338 \pm 0.007(stat)$ respectively.

More details on particle identification for the pre-selected events are shown in Table 2. The numbers of tracks surviving the preselection criteria are shown in row 1. The numbers of electron and muon candidates identified in the data sample are compared to those of the Monte Carlo simulated backgrounds in rows 2 and 3. Proton candidates shown in row 4 are due to the mis-identification of (~ 0.5 %) the pre-selected charged leptons before imposing the final $d\mathrm{E}/d\mathrm{x}$ requirement. This was anticipated because:

† a high energy muon or electron can sometimes deposit a great deal of its energy inside the calorimeters due to bremsstrahlung, e^+e^- pair production, or deep inelastic nuclear interaction (DIS). These processes are characterized by large uncertainties, small cross sections, hard spectra, and large energy fluctuations in the generation of electromagnetic and hadronic showers,

† a high energy lepton can undergo DIS in the ECAL, where only the electromagnetic component of the shower is measured by the lead glass, resulting in $E_{ECAL} < 35\,\mathrm{GeV}$,

† hadrons are emitted in τ decays.

These effects, in particular the DIS of the e's and μ's, made the proton identification, with E_{tot} cuts alone, difficult. However, after removing the identified e^+e^- and $\mu^+\mu^-$ pairs, the final $d\mathrm{E}/d\mathrm{x}$ requirement efficiently eliminated every one of the 1249 identified proton candidates in the data. The 1.2 background events, all identified as $Z^0 \to \mathrm{p}+\mu$, consisted of 0.5 events coming from $\mu^+\mu^-$ and 0.7 events from $\tau^+\tau^-$. The $\mu^+\mu^-$ background events can be understood as DIS of one of the high energy muons, while the $\tau^+\tau^-$ background events are due to mis-identification of $Z^0 \to \tau_1\tau_2$, where $\tau_1 \to h$ and $\tau_2 \to \mu$.

Allowing the $d\mathrm{E}/d\mathrm{x}$ and E_{tot} cuts to vary, based on the analysis of the Monte Carlo simulated events, we estimated a 0.71 % systematic uncertainty for the detection of the signal.

Final-state radiation (FSR) is expected to be different for muons and electrons or protons. Changing the particle code from μ to e in the final-state of $Z^0 \to \mu^+\mu^-$ events (see section 3) may have caused an underestimation of the FSR correction on the electrons in the $Z^0 \to$ pe events resulting in a larger than expected acceptance of the signal. Based on a study of the $Z^0 \to e^+e^-$ events, we found that 0.47 % of the electrons could have a measured E_{ECAL} less than 35 GeV. This value was quoted as the systematic uncertainty in the estimation of the detection efficiency due to FSR.

Another source of systematic error came from the 0.41 % uncertainty in the collected luminosity [19]. In summary, a quadratic sum of all of the above mentioned errors yielded a 0.94 % systematic error on the detection efficiency, ϵ_{pe}, and 0.81 % on $\epsilon_{\mathrm{p}\mu}$.

7 Results and conclusion.

Using a data sample of 5.2 million Z^0 decays and with 0 candidate event found, we obtained the following upper limits:
$$\Gamma(Z^0 \rightarrow \text{pe}) = 4.6 \,\text{keV}$$

and

$$\Gamma(Z^0 \rightarrow \text{p}\mu) = 4.4 \,\text{keV}$$

at 95 % confidence level [21].

This is the first time that limits have been obtained on the partial widths of Z^0 decays for processes which simultaneously violate baryon-, lepton-, and fermion-number conservation. The above limits are comparable to the existing limits on lepton family number violating Z^0 decays [8].

References

[1] A.G. Cohen, D.B. Kaplan and A.E. Nelson, Annu. Rev. Nucl. Part. Sci. **43** (1993) 27; See also A.D. Dolgov, Proceedings of the 3rd Int. Workshop on Theoretical and Phenomenological Aspects of Underground Physics, Gran Sasso, INFN, Italy 19–23 Sept. 1993(TAUP 93) page 28, edited by C. Arpesella, E. Bellotti and A. Bottino.

[2] G. 't Hooft, Phys. Rev. Lett. **37** (1976) 8; G. 't Hooft, Phys. Rev. **D14** (1976) 3432.

[3] E.W. Kolb and M.S. Turner, The Early Universe, Addison-Wesley, Reading, Mass. (1990) and references therein.

[4] A.D. Sakharov, JETP Lett. **6** (1967) 6.

[5] V.A. Kuzmin, V.A. Rubakov and M.E. Shaposhnikov, Phys. Lett. **B155** (1985) 36; F. Klinkhamer and N. Manton, Phys. Rev. **D30** (1984) 2212.

[6] P. Arnold and L. McLerran, Phys. Rev. **D37** (1988) 1020; L. Carson *et al.*, Phys. Rev. **D42** (1990) 2127.

[7] R.M. Barnett *et al.*, Phys. Rev. **D45** (1996) S1.

[8] OPAL Collab., R. Akers *et al.*, Z. Phys. **C67** (1995) 555; ALEPH Collab., D. Decamp *et al.*, Phys. Rep. **216** (1992) 253; DELPHI Collab., P. Abreu *et al.*, Z. Phys. **C73** (1997) 243; L3 Collab., O. Adriani *et al.*, Phys. Lett. **B316** (1993) 467.

[9] OPAL Collab., K. Ahmet *et al.*, Nucl. Instr. and Meth.**A305** (1991) 275; P.P. Allport *et al.*, Nucl. Instr. and Meth.**A324** (1993) 34; P.P. Allport *et al.*, Nucl. Instr. and Meth.**A346** (1994) 476.

[10] M. Hauschild *et al.*, Nucl. Inst. Meth. **A314** (1992) 74. M. Hauschild, Nucl. Inst. Meth. **A379** (1996) 436.

[11] H.M. Fisher *et al.*, Nucl. Inst. Meth. **A252** (1986) 331.

[12] B.E. Anderson *et al.*, IEEE Transactions on Nuclear Science **41** (1994) 845.

[13] OPAL Collab., G. Alexander *et al.*, Z. Phys. **C52** (1991) 175; OPAL Collab., R. Akers *et al.*, Z. Phys. **C61** (1994) 19.

[14] G. Marchesini *et al.*, Comp. Phys. **67** (1992) 465; S. Jadach *et al.*, Comp. Phys. Comm. **66** (1991) 276.

[15] J. Allison *et al.*, Nucl. Instr. Meth. **A317** (1992) 47.

[16] M. Böhm, A. Denner and W. Hollik, Nucl. Phys. **B304** (1988) 687; F.A. Berends, R.R. Kleiss and W. Hollik, Nucl. Phys. **B304** (1988) 712.

[17] T. Sjöstrand and M. Bengtsson, Comp. Phys. Comm. **82** (1994) 74; T. Sjöstrand, CERN-TH.6488/92; T. Sjöstrand, LUTP 95-20.

[18] OPAL Collab., M.Z. Akrawy *et al.*, Phys. Lett. **B235** (1990) 379.

[19] OPAL Collab., R. Akers *et al.*, Z. Phys. **C61** (1994) 19.

[20] C.Y. Chang *et al.*, Nucl. Instr. Meth. **A264** (1988) 194.

[21] R.D. Cousins and V.L. Highland, Nucl. Instr. Meth. **A320** (1992) 331. Following this ref. we have, within the Bayesian framework, incorporated the systematic errors into the detection efficiencies for the calculation of the 95 % confidence level of the upper limits.

		Data Collected in 1990-1994	Monte Carlo					
			Background				signal	
			(e^+e^-)	$(\mu^+\mu^-)$	$(\tau^+\tau^-)$	total	(p,e)	(p,μ)
1.	Sample size used in analysis	119 (pb^{-1})	252 (pb^{-1})	463 (pb^{-1})	345 (pb^{-1})		10,000 (events) 100 %	10,000 (events) 100 %
2.	Multiplicity and Status requirements	1,896,853	440,027	148,053	141,117	729,197	92 %	93 %
3.	preselection	139,328	73,855	65,436	149	139,440	48 %	50 %
4.	Particle identification	135,679 *(identified as*	73,797	61,807	84 $Z^0 \to e^+e^-$,	135,688	13 % *or*	14 % $\mu^+\mu^-$*)*
		0 *(*	0 *identified*	0.5	0.7 *as*	1.2	33.8 % *signal*	35.3 % *)*

Table 1: *Comparison of event flows for data and Monte Carlo simulated events. Numbers shown in rows 2, 3 and 4 represent events surviving the selection criteria. The Monte Carlo background event numbers were normalized to the luminosity of the data.*

	Data Collected in 1990-1994	Monte Carlo Background			
		(e^+e^-)	$(\mu^+\mu^-)$	$(\tau^+\tau^-)$	total
preselection	278,656	147,710	130,872	298	278,880
Electron candidates	147,527	147,467	93	151	147,711
Muon candidates	124,996	3	125,142	41	125,186
Proton candidates	1,249	53	914	78	1,045
Proton identified	0	0	0.5	0.7	1.2
			as	$Z^0 \rightarrow \mu + p$	

Table 2: *Comparison of track flows for data and Monte Carlo simulated events during particle identification. Numbers shown in the Table give the number of tracks surviving the selection criteria.*
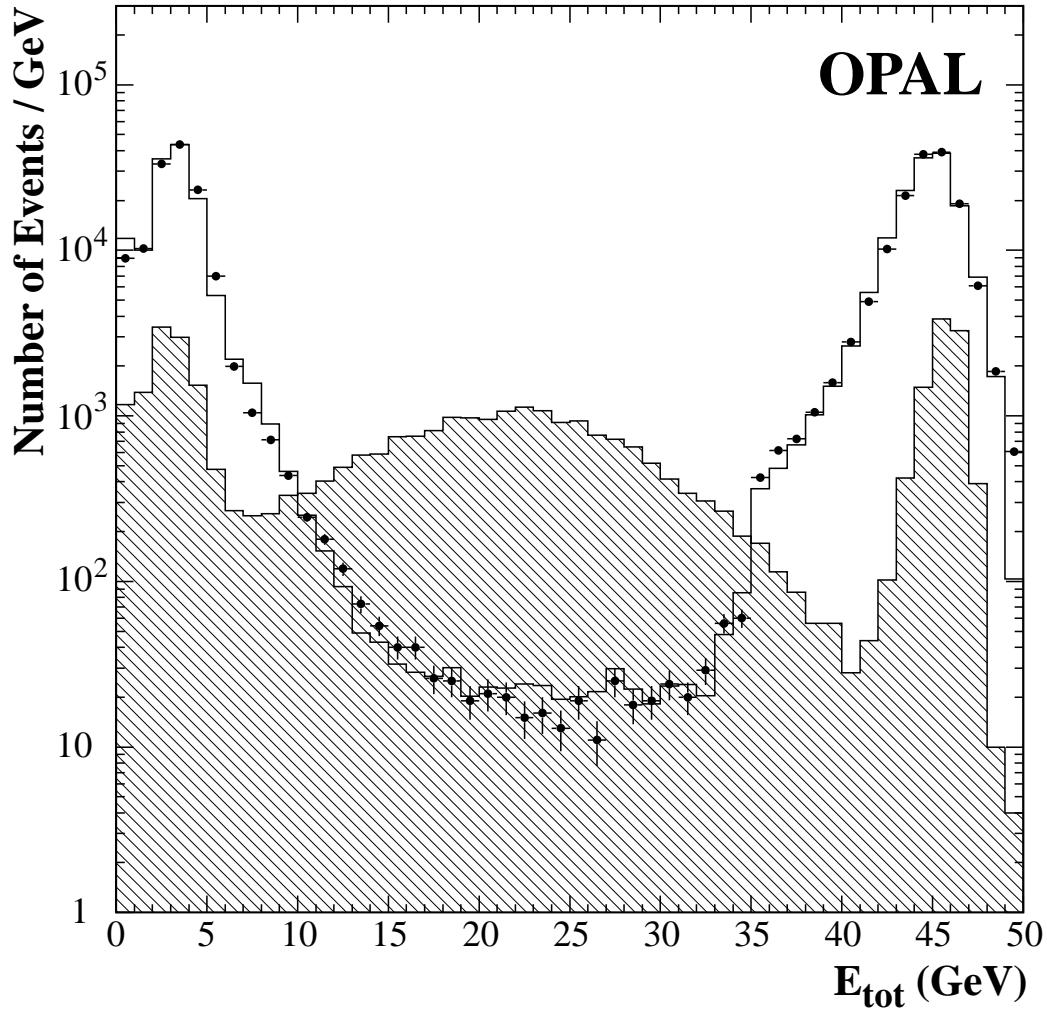
Figure 1: *The measured calorimeter energy (data points), E_{tot}, associated with each well measured charged track satisfying the event preselection criteria for the data. The Monte Carlo simulated $\mu^+\mu^-$, e^+e^-, and $\tau^+\tau^-$ events are shown by the open histogram for comparison. The shaded histogram represents the Monte Carlo simulated $Z^0 \rightarrow pe/p\mu$ decays with arbitrary normalization.*
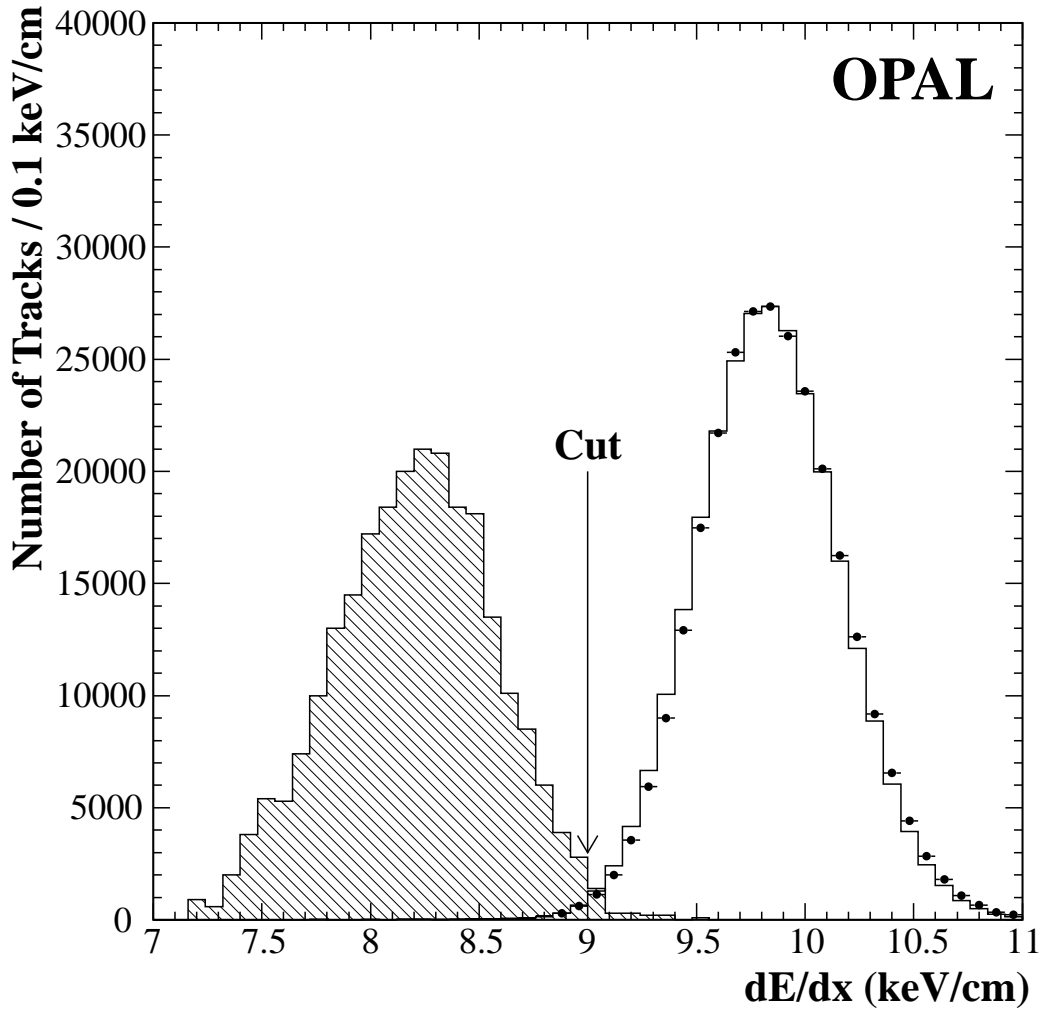
Figure 2: *The distribution of specific ionization energy loss, $d\mathrm{E}/dx$, of the well measured charged tracks (data points) that survived the event preselection. The open histogram shows the corresponding distribution for the Standard Model Monte Carlo simulated background charged lepton pairs. The $d\mathrm{E}/dx$ distribution of a 45 GeV proton which survived the same selection criteria is shown as the shaded histogram with arbitrary normalization.*

16